Free Piston Compressor with a Variable Volume Ratio: Insights on Modeling Approach and Control Strategy

Conference Paper · July 2018

CITATIONS
0

READS
23

4 authors, including:

Sergei Gusev
Ghent University
20 PUBLICATIONS **138** CITATIONS
SEE PROFILE

Davide Ziviani
Purdue University
53 PUBLICATIONS **271** CITATIONS
SEE PROFILE

Michel De Paepe
Ghent University
280 PUBLICATIONS **2,960** CITATIONS
SEE PROFILE

Free Piston Compressor with a Variable Volume Ratio: Insights on Modeling Approach and Control Strategy

Sergei GUSEV[1*], Heinz VERVAEKE[2], Davide ZIVIANI[3], Michel DE PAEPE[4]

[1]Ghent University, Department of Flow, Heat and Combustion Mechanics,
Graaf Karel De Goedelaan 5, 8500 Kortrijk, Belgium
Contact Information (Servei.Gusev@UGent.be)

[2]Ghent University, Department of Electrical Energy, Systems and Automation,
Graaf Karel De Goedelaan 5, 8500 Kortrijk, Belgium
Contact Information (Heinz.Vervaeke@UGent.be)

[3]Ray W. Herrick Laboratories, Purdue University
177 S Russell Street, West Lafayette, IN, 47907-2099, USA
Contact Information (DZiviani@Purdue.edu)

[4]Ghent University, Department of Flow, Heat and Combustion Mechanics,
Sint-Pietersnieuwstraat 41, 9000 Ghent, Belgium
Contact Information (Michel.DePaepe@UGent.be)

* Corresponding Author

ABSTRACT

Increasing requirements to heat pump performance ratings as well as pressing environmental concerns force manufacturers to evaluate the potential of natural refrigerants such as ammonia, propane or carbon dioxide, and implement advanced cycle architectures. Beside the use of the appropriate working fluid, the compressor should have ideally an optimal built-in volume ratio (BVR) for any pressure ratio during its operation. Practically, such mode of operation is only possible if the BVR can be made adjustable in real time in order to follow pressure fluctuations due to possible variable heat pump loads. The concept of such a machine with an embedded linear alternator has been developed and patented. The rotation of the piston is used to adjust the timing of the ports so that, after the compression, the pressure in the cylinder is equal to the required one in the discharge line. The intake port has been designed in such a way, that it remains open during the suction phase. Therefore, no pressure difference is needed to actuate the ports and throttling losses can be nearly avoided. The reciprocating movement of the piston used to compress the working fluid is fully controlled which eliminates the need of springs typically used in similar machines. The dead volume of this machine is only defined by the machining tolerances, so it can be made extremely small allowing high pressure ratios. A test setup is used to validate the theoretical model and investigate the influence of the key parameters of the machine.

1. INTRODUCTION

Position control of moving bodies is a challenging task if both high accuracy and dynamics are required. In various applications, it is important to bring a mass not only to a desired position but also within a strict time span. A model predictive control approach is widely used in order to improve the positioning of such systems. Modeling implies the definition of all forces acting on a moving mass. Therefore, the speed and the acceleration must be measured or calculated, and included into a control algorithm, accordingly. In particular, the frictional force is mainly dependent on the velocity and the inertia force is the function of the mass acceleration. Depending on the situation, various sensors can be used: encoders, accelerometers etc. However, it is not always possible to measure all required signals, hence the missing information must be obtained from numerical simulations. For instance, by taking first and second derivatives of the position signal, the velocity and the acceleration can be estimated, as reported in Merry et al. (2010); Belanger et al. (1998); Aguado-Rojas et al. (2017). In other cases, a reversed calculation is required: the position and the velocity

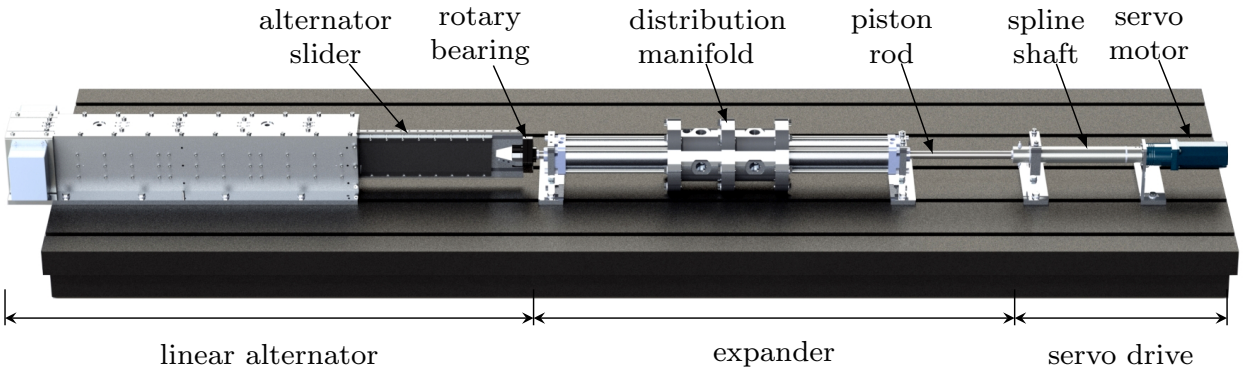

Figure 1: View of the test setup with separated linear and rotary motion.

are obtained by integrating the acceleration readings (Lotfi & Huang, 2016). When possible, both acceleration and displacement signals can be used in order to improve the accuracy of the control, as outlined by Kim et al. (2014). Nevertheless, noise is always present in the signals acquired from the sensors, which not necessarily originates from an electromagnetic interference but from a random error generated by the sensor itself. This error, propagating through calculations of a control algorithm, can drastically affect the positioning, therefore, a signal conditioning is almost always used. Several signal conditioning methods are described in literature e.g., (Jenkins & Hilkert, 2008).

How successful a signal conditioning can be, it is defined by the right choice of a filtering method but this choice is not evident. Some information about the signal being filtered is very useful. In particular, by knowing the expected frequency and the amplitude of the signal, an excessive smoothing can be avoided since it might not only remove the noise but also distort the information being analyzed. For instance, widely used moving average method generates a result which is delayed in respect to the filtered signal (Smith, 1997). In the case of a model predictive control of a high dynamic system, any time lag in the control chain is obviously unwanted. A method producing no phase shift is Zero-phase filtering, which implies an averaging of a signal smoothed in a straight and a reverse direction. This method is incorporated in the favored scientific software[1, 2] and it can be recommended for the data post-processing. However, real time calculations require another solution since there is no information from the future available. A good alternative is the Savitzkiy-Golay filter (Savitzky & Golay, 1964) using a limited acquired data window and, therefore, producing a very small phase shift but at the same time generating a good smoothed result. In this paper, the analysis of the experimental data will be provided as well as some related issues affecting the control algorithm.

2. TEST SETUP DESCRIPTION

A Free-Piston Linear Expander (FPLE) with variable internal volume ratio and its working principle were first introduced and explained in (Gusev, Ziviani, et al., 2016; Gusev, Hernandez, et al., 2016). Successively, this device is also patented Gusev (2016). The machine can act as a compressor and the operation mode can be switched on the fly by changing the rotation direction. In order to design and validate models needed for the control system development, a test setup has been built and it is shown in Figure 1. The linear motion is separated from rotational motion in order to facilitate the study of both. The translation of the piston is realized by a linear motor/alternator (LMA). This device is assembled from standard industrial components in a custom-designed housing containing a linear guiding system. The LMA comprises of two iron core coils placed opposite of each other, a sliding frame with back-to-back attached magnetic sections is supported by linear bearings. The slider is connected to the compressor through a bearing which decouples the rotation of the piston shaft. This connection is rigid since contains no elastic parts. Two magnetic encoders, installed from the both sides of the slider, provide the linear position feedback signal. The rotation is provided by a servo motor with a gearbox. A spline shaft separates the piston translation from the motor, providing the rotation only.

[1] `https://nl.mathworks.com/help/signal/ref/filtfilt.html`
[2] `https://docs.scipy.org/doc/scipy-0.14.0/reference/generated/scipy.signal.filtfilt.html`

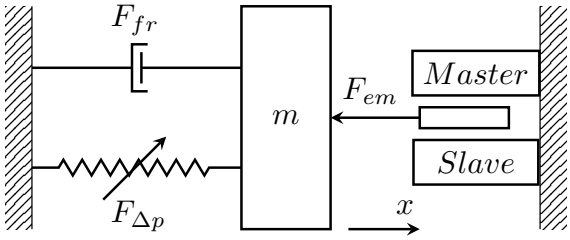

Figure 2: The lumped model of the linear system.

The motors used in the current setup are of iron core synchronous permanent magnet type. The three-phase windings shares the same laminated iron core. The permanent magnets are attached to the back plates with a step of 0.012 m and skewed with the angle of 88 degree. Skewing reduces the cogging effect but also reduces the efficiency of the motor.

Both motors are connected to their own drive. One motor is configured as master. Position setpoints are recalculated into the force setpoints which are transferred to the slave motor directly. This motor does not receive a position feedback and it operates therefore in a slave mode.

Each motor is provided with its own incremental magnetic encoder with a sinusoidal output voltage (1 V_{PP} or volt peak-to-peak). 1 stands for the voltage difference between the lowest and the highest amplitude point. More information about the working principle and the signal processing can be found in literature[3].

While the magnets of a secondary section move along the encoder, a sinusoidal signal is generated which corresponds with the magnets pattern. The distance between two consecutive north poles of the secondary section defines the full period of the sensor signal. The sensor discrepancy, declared by the manufacturer, is 0.1 mm.

Magnetic encoders are highly immune to contamination in an industrial environment. Therefore, electromagnetic encoders provide very robust measurements. However, special attention is needed when incremental encoders are used. For instance, the position reading is only certain within a magnet pitch but not within the full stroke length. Therefore, zeroing is required after a signal interruption due to i.e. a power failure or at the start up. This procedure is realized by slowly moving the piston until its extreme position and detecting the rising current when the piston is stopped.

3. SYSTEM IDENTIFICATION

The key to success in obtaining the needed volume ratio is a development of a certain piston movement profile which can be reproduced by the machine. Therefore, this profile must be transformed into forces and torques applied to the moving mass and used as setpoints for a feed-forward signal. Obviously, these forces and torques must not exceed the machine's structural limits. In order to identify the system forces, which can not be measured directly, such as frictional force, the piston velocity must be calculated. By knowing the mass of the moving parts and the maximum of the forces acting on the piston, the maximum acceleration can be estimated. If necessary, the position profile can be adjusted.

By referring to the schematic of the mechanical system model shown in Figure 2, the dynamics of the moving mass, m, is defined by Newton's Second Law and it can be expressed as follows:

$$F_{\Delta p} - F_{fr} - F_{em} = m\frac{d^2x}{dt^2}, \tag{1}$$

where $F_{\Delta p}$ is the gas force created by the pressure difference in the compressor, F_{fr} is the frictional force, and F_{em} is the electromagnetic force applied by the master and the slave linear motor sections.

[3] http://www.ti.com/lit/ug/tidua05a/tidua05a.pdf

3.1 Gas force

In order to include the gas force into the model, the pressure in both working chambers is measured and logged. By knowing the geometry of the device, the gas force can be calculated as expressed:

$$F_{\Delta p} = \Delta p \frac{\pi (D_{cyl}^2 - D_{rod}^2)}{4}, \tag{2}$$

where Δp is the pressure difference, D_{cyl} is the cylinder internal diameter, and D_{rod} is the rod diameter.

3.2 Frictional force

The frictional force is estimated by adopting the model proposed by Bo & Pavelescu (1982):

$$F_{fr} = \left(F_c + (F_s - F_c) e^{-(|v_{ps}/v_s|)^{\zeta}} + F_v |v_{ps}/v_s| \right) sgn(v), \tag{3}$$

where F_s is the static friction force, F_c is the Coulomb friction force and F_v is the viscous friction force. v_s is a speed limit for Stribeck friction, ζ is the empirical coefficient, and $sgn(v)$ is the function extracting the sign of the velocity value. This set of equations is also used for the rotation by substituting the angular parameters instead of the linear ones and the inertia moment instead of the mass.

4. EXPERIMENTAL WORK

The translation and the rotation of the piston must be fully controlled with minimal deviations in order to ensure their synchronization. The trajectories define the machine inlet/outlet timing and therefore are vital for a proper functionality. First test campaign has been performed with closed ports and was focused on the system identification. At the same time, the thermodynamic model has been validated. More specifically, the pressure build-up was simulated using the same force as a function of time similarly to the experiments. The piston was accelerated until a certain speed and then stopped at different positions. In such a way a pressure from 3 to 7 bar was created. After the piston was stopped, the pressure started to equalize with the ambient. The leakage model has been compared with this part of the experiments. Both have shown a good agreement between the modeled and experimental results.

The second experimental campaign has been carried out in a continuous mode by combining the previously used velocity profile with the piston rotation. Both the translation of the piston and its rotation were synchronized, so the actual operation of the device was approached. Several pressure ratios (PR) have been obtained and analyzed as depicted in Figure 3.

Both experimental campaigns revealed several problems with the positioning accuracy at high linear speeds. All efforts to improve the positioning accuracy by means of the controller settings (PI-controller) led to a self-excitation of the control loop manifesting in a vibrations and sound even when the slider was not moving. The frequency measured was about 400 Hz, which corresponds with a period of 2.5 milliseconds.

4.1 Sources of the uncertainties

During the commissioning, the motor has been configured according to Master/Slave approach. This approach is still widely used in industry if the requirements to the positioning are moderate, regardless the fact that this method has been proposed when the first dual arm robots carrying a load or portal cranes and mills appeared. At that time, the major drawbacks were immediately figured out and some remedy have been proposed (Perez-Pinal et al., 2004). In such closed loop systems, both manipulators or motors are connected through an object being moved or a common beam. Any asynchronism in such a system leads to undesired or even potentially dangerous tensions in the object and the manipulators. The power consumption of servo motors operating under these conditions is higher than normal since they need to overcome forces or torques which ideally should not appear. The positioning accuracy is also affected: the response of the slave part operating under force/torque control is slow in respect to the system dynamics.

In the current setup, the force signal from the master section is being sent simultaneously to the master power electronics and to the slave drive. The latter needs some time to process the signal and to send it to its power electronics. This

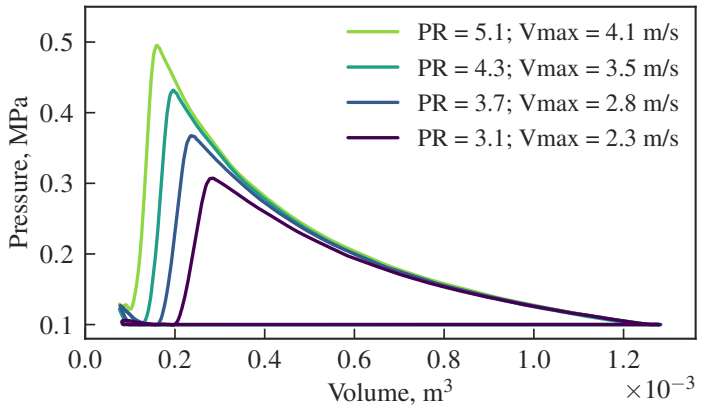

Figure 3: Different compression ratios.

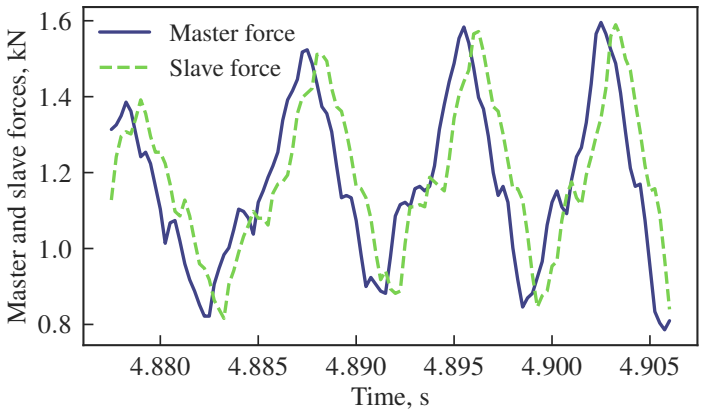

Figure 4: Asynchronism of master and slave forces.

leads to a certain time lag of the slave force or torque. This lag can be figured out by comparing both signals either graphically or, more general, by applying an analytical algorithm involving the Fast Fourier Transformation (FFT)[4]. This has been performed the following way:

- One full period has been extracted from the log file by peak detection of the position signal[5].
- Both signals have been Fourier-transformed by means of the *fft* function included in *scipy.fftpack*[6].
- The slave signal has been inverted and conjugated.
- The reversed Fourier transformation has been applied to the product of both resulting transformed signals.

The result of these manipulations is the number of steps in the log file, with which one signal is shifted relatively to another one. By multiplying this value with the time step, the time delay can be calculated. As it can be seen in Figure 4, a very constant lag of 0.75 milliseconds was figured out, which is apparently related to the system cycle time. This time lag leads to a quite significant difference in the master and slave forces, especially when they change rapidly. Figure 5 illustrates that the difference exceed sometimes ±0.7 kN, while the variation of the sum of both forces is maximum ±10 kN. This phenomenon is very undesirable in the vicinity of the dead points, since the positioning requirements in

[4] `https://stackoverflow.com/questions/4688715/find-time-shift-between-two-similar-waveforms`
[5] `https://github.com/samyachour/EKG_Analysis/blob/master/detect_peaks.py`
[6] `https://docs.scipy.org/doc/scipy/reference/fftpack.html`

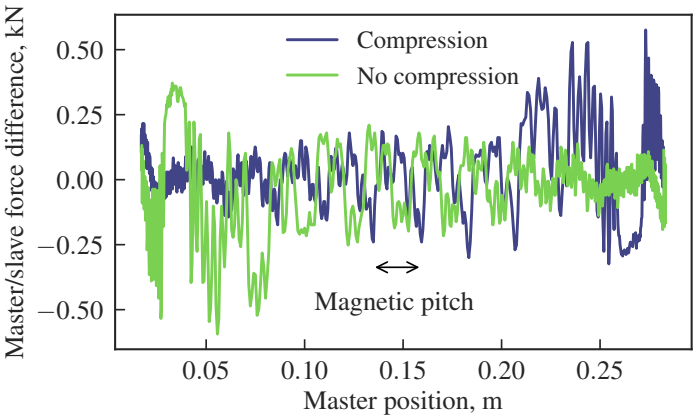

Figure 5: Master and slave force difference.

these zones in very high. Furthermore, an asymmetric attraction force causes a higher friction in the guiding system and therefore decreases the system efficiency and the life time. Beside that, the hardware imperfection can lead to similar effects.

The problem mentioned above can be eliminated by using advanced control algorithms, since it originates from solely software and drive configuration. In the future, the force setpoint will be sent to both drives simultaneously from an external control routine when it is ready to use.

4.2 Correction of systematic errors

Further investigation is required in order to map systematic error sources. For instance, any dissimilarities of the motors geometry caused by manufacturing imperfections can cause to a sine-error. Sine error can be calculated as follows:

$$F_{dif} = F_{em} \sin\left(2\pi \frac{D_{dif}}{MP_{n-n}}\right), \tag{4}$$

where F_{dif} is the force difference between the two motors, F_{em} is the force generated by the motors, D_{dif} the length of misalignment and MP_{n-n} the north-to-north magnetic pitch.

Another potential source of systematic primary error which propagates through the calculation, are the encoders. Therefore, the evaluation of the sensor readings is required before the system control design. Since no reference encoder was available, the difference between both the master and the slave sensor readings has been analyzed and it is depicted in Figure 6. In this experiment, the piston oscillated between the left and the right dead points, driven by the LMA and compressing air in the right working chamber. The difference with a very clear pattern and a step corresponding with a magnetic pitch, was larger during the piston movement from left to right but no influence of the pressure inside the working chamber was found. By mapping the linear dependency of the measured difference in function of the piston position and by applying a correction coefficient for the velocity, a first step to a better position acquisition can be made.

4.3 Random noise filtering

As aforementioned, each sensor signal contains some random noise. If a velocity or an acceleration are obtained from a noisy position signal, both are significantly distorted since the signal-to-noise ratio is degraded with each derivation. The average velocity can be calculated from two sequential position measurements x_i and x_{i+1} as follows:

$$v = \frac{x_{i+1} - x_i}{\Delta t}, \tag{5}$$

where Δt is the sampling time.

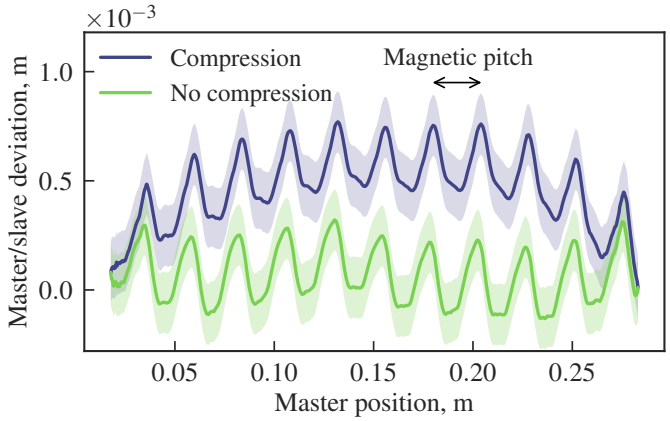

Figure 6: Difference between readings of master and slave encoders.

The uncertainty in time measurement can be neglected. Therefore, the error in piston velocity δv estimation is solely the function of the encoder uncertainty $\delta x = f(v,x)$. The following statement is then legal:

$$(\delta v)^2 = \frac{(\delta x_{i+1})^2 + (\delta x_i)^2}{(\Delta t)^2}. \tag{6}$$

By analyzing Equation 6, one can come to the conclusion that the shorter acquisition period, Δt, will cause a larger error in velocity than at a smaller Δt, however, a larger sampling window will result in a larger time delay.

In order to figure out whether a delay in the used velocity signal persists and to quantify it, the velocity feedback signal from the drive has been compared with a first derivative of the position signal. The position signal was filtered by Savitzky-Golay filter. Figure 7 presents the results of this comparison. According to the calculations, the velocity signal from the drive is 8.5 ms delayed in respect to the calculated signal.

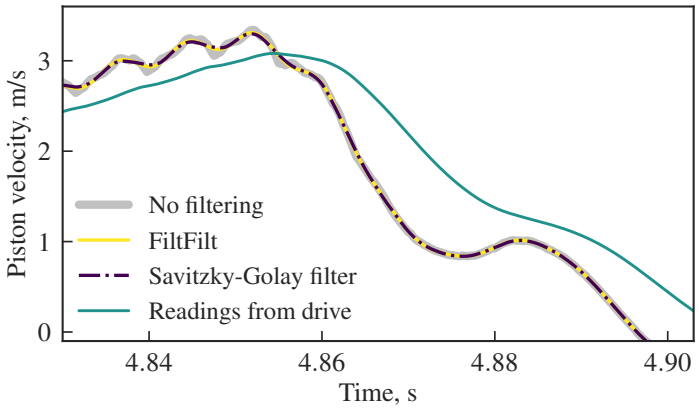

Figure 7: Illustration of various velocity calculation and filtering algorithms.

Being the second derivative of the position signal, the acceleration signal is even more affected by the encoder random errors as it can be seen in Figure 8. In the proposed design, the use of an accelerometer is hardly possible, so the only option to include the acceleration signal in the control algorithm is to estimate it from the properly filtered position signal. The force signal measured by the drive gives the reference for this estimation. Since the mass of the moving parts can be measured very accurately, the acceleration is than the ratio of the sum of all forces acting on the piston and the total moving mass.

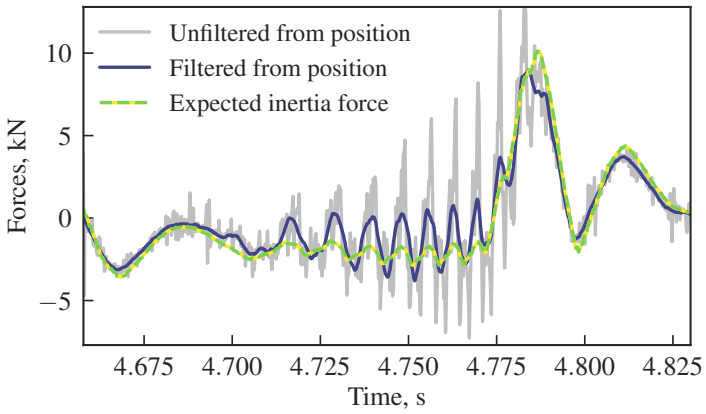

Figure 8: Force estimation from position signal.

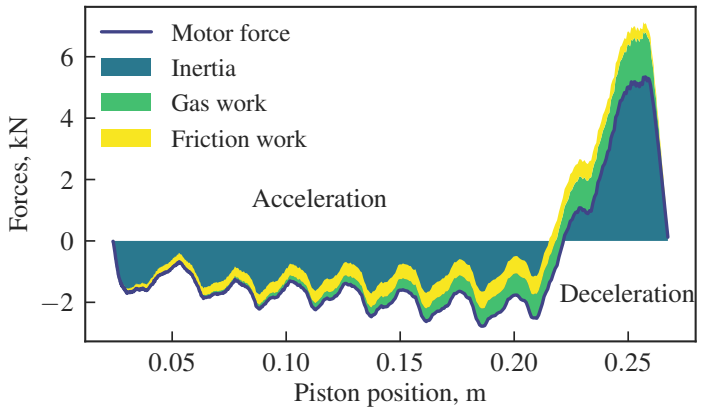

Figure 9: Energy transformation during one stroke.

The thrust force and the gas force can be measured directly, the friction force can be identified as a function of the piston speed and, therefore, the inertia force can be estimated. By comparing the inertia force obtained from the filtered position signal with the estimated one and by minimizing the phase shift, the filtering settings can be optimized.

5. EFFICIENCY ASSESSMENT

During these test runs, the piston has performed several reciprocating cycles for each selected speed. Due to an increasing overshoot, the piston travel length and the volume ratio also increased. A relatively low pressure build-up can be explained by the leakages, which are more significant at relatively low piston speeds. The major difficulty of the evaluation of the compressor unit in the current setup is a limited robustness of the machine. This was never meant to operate in steady state for a long period of time. Furthermore, the control of the piston motion was not optimized at the moment of this experimental campaign. The authors needed to proceed carefully figuring out the major limits and preserving the machine from damage.

The work provided by the motor is used to overcome the friction losses and the gas force. The excess is accumulated as inertia and released back during the piston deceleration as it depicted in Figure 9. The piston movement profile optimization results in maximization the green zone in the right part of the plot, which means that all work of the motor is transferred to the compression process by using the inertia of the moving piston.

6. CONCLUSIONS

The dynamics of the piston must be optimized according to the used linear generator. There is a trade-off between the high dynamics of the piston movement and a relatively high static force, which is typical for the piston extreme positions. The crucial requirement is that the piston position must be controlled by the generator electronics at any moment.

The major difference with most similar systems is that in the current setup the piston is not moving freely but, instead, its movement is fully controlled, so there are no bouncing devices needed. This approach provides a potentially more efficient way to transform the electrical energy into compression work since losses in bouncing devices are avoided.

The proposed model predictive control strategy implies an accurate position feedback which is needed for a real time estimation of the forces acting on the piston. Savitzkiy-Golay filter applied to the position signal provides the results comparable with non-real time zero-phase filters and prevents a delay of the filtered signals.

This setup has the advantage of testing various linear compressors and expanders with different sizes, by easily replacing generators and motors to study the dynamics of the whole system. The piston movement can be matched to the maximum efficiency range of the generator used.

NOMENCLATURE

Acronyms		
BVR	Built-in Volume Ratio	
FPLE	Free-Piston Linear Expander	
LMA	Linear Motor/Alternator	
MP	Magnetic Pitch	
PR	Pressure Ratio	
Latin		
D	diameter	(m)
F	force	(N)
m	mass	(kg)
p	pressure	(Pa)
t	time	(s)
V	volume	(m^3)
v	speed	(m/s)
x	displacement	(m)
Greek		
Δ	difference	(-)
δ	Deviation	(-)
ζ	Empirical coefficient	(-)
Subscript		
c	Coulomb	
cyl	cylinder	
dif	difference	
em	electromagnetic	
fr	friction	
n-n	north-to-north	
p	pressure	
ps	piston	
rod	rod	
s	static	
v	viscous	

REFERENCES

Aguado-Rojas, M., Pasillas-Lépine, W., Loría, A., & Bernardinis, A. D. (2017). Angular velocity estimation from incremental encoder measurements in the presence of sensor imperfections. *IFAC-PapersOnLine*, *50*(1), 5979 - 5984. (20th IFAC World Congress) doi: 10.1016/j.ifacol.2017.08.1260

Belanger, P., Dobrovolny, P., Helmy, A., & Zhang, X. (1998). Estimation of angular velocity and acceleration from shaft-encoder measurements. *The International Journal of Robotics Research*, *17*(11), 1225-1233. doi: 10.1177/027836499801701107

Bo, L. C., & Pavelescu, D. (1982). The friction-speed relation and its influence on the critical velocity of stick-slip motion. *Wear*, *82*(3), 277 - 289. doi: 10.1016/0043-1648(82)90223-X

Gusev, S. (2016, December 15). *Free piston device.* Google Patents. (WO Patent App. PCT/EP2016/063, 223)

Gusev, S., Hernandez, A., Ziviani, D., & van den Broek, M. (2016). Modeling of a variable-BVR rotary valve free piston expander/compressor. In *Latin american conference on automatic control* (pp. 42–48). Medellin, Colombia.

Gusev, S., Ziviani, D., De Viaene, J., Derammelaere, S., & van den Broek, M. (2016). Modelling and preliminary design of a variable-BVR rotary valve expander with an integrated linear generator. In *23rd international compressor engineering conference* (p. 10).

Jenkins, S. T., & Hilkert, J. M. (2008, 2008). Sin/cosine encoder interpolation methods: encoder to digital tracking converters for rate and position loop controllers. In *Proceedings of SPIE - the International Society for Optical Engineering.* Bellingham, Wash.: Society of Photo-optical Instrumentation Engineers.

Kim, J., Kim, K., & Sohn, H. (2014). Autonomous dynamic displacement estimation from data fusion of acceleration and intermittent displacement measurements. *Mechanical Systems and Signal Processing*, *42*(1), 194 - 205. doi: 10.1016/j.ymssp.2013.09.014

Lotfi, B., & Huang, L. (2016). An approach for velocity and position estimation through acceleration measurements. *Measurement*, *90*, 242 - 249. doi: 10.1016/j.measurement.2016.04.011

Merry, R., van de Molengraft, M., & Steinbuch, M. (2010). Velocity and acceleration estimation for optical incremental encoders. *Mechatronics*, *20*(1), 20 - 26. (Special Issue on "Servo Control for Data Storage and Precision Systems", from 17th IFAC World Congress 2008) doi: 10.1016/j.mechatronics.2009.06.010

Perez-Pinal, Nunez, C., Alvarez, R., & Cervantes, I. (2004, Nov). Comparison of multi-motor synchronization techniques. In *30th annual conference of ieee industrial electronics society, 2004. iecon 2004* (Vol. 2, p. 1670-1675 Vol. 2). doi: 10.1109/IECON.2004.1431832

Savitzky, A., & Golay, M. J. E. (1964). Smoothing and differentiation of data by simplified least squares procedures. *Analytical Chemistry*, *36*(8), 1627-1639. doi: 10.1021/ac60214a047

Smith, S. W. (1997). *The scientist and engineer's guide to digital signal processing.* San Diego, CA, USA: California Technical Publishing.